Available online at www.sciencedirect.com

ScienceDirect

Advances in Space Research 60 (2017) 1827–1837

ADVANCES IN SPACE RESEARCH (a COSPAR publication)

www.elsevier.com/locate/asr

Salient features of the dayside low latitude ionospheric response to the main phase step-I of the 17 March 2015 geomagnetic storm

Mala S. Bagiya [a,*], A.S. Sunil [a], D. Chakrabarty [b], Surendra Sunda [c]

[a] Indian Institute of Geomagnetism (DST), Navi Mumbai 410218, India
[b] Physical Research Laboratory, Ahmedabad 380009, India
[c] Space Application Center, Ahmedabad 380053, India

Received 1 April 2017; received in revised form 23 May 2017; accepted 5 June 2017
Available online 13 June 2017

Abstract

Based on TEC observations by India's GPS Aided GEO Augmented Navigation (GAGAN) GPS network, we report the dayside low latitude ionospheric variations over the Indian region during the moderate main phase step-I of the 17 March 2015 geomagnetic storm. In addition, we assess the efficacy of GPS inferred TEC maps by International GNSS service (IGS) in capturing large scale diurnal features of equatorial ionization anomaly (EIA) over the Indian region during this period. Following the prompt penetration electric field (PPE) at ~0605 UT, equatorial electrojet (EEJ) enhances by ~55 nT over 75 ± 3°E longitudes where main phase step-I is coincided with local noon. Initial moderate EIA gradually strengthens with the storm commencement. Although GAGAN TEC exhibits more intense EIA evolution compare to IGS TEC maps, latitudinal extent of EIA are comparable in both. The enhanced EEJ reverses by ~0918 UT under the effect of overshielding electric field, the later is accompanied by northward turning of interplanetary magnetic field (IMF) Bz. The weakening of well evolved EIA reflects in IGS TEC maps after ~45 min of the overshielding occurrence. In contrary, GAGAN TEC shows the corresponding feature after ~0115 h. Resurgence of EIA, following the PPE ~1115 UT, shows up in GAGAN TEC but IGS TEC maps fails in capturing this feature. The observed low latitude TEC variations and EIA modulations are explained in terms of the varying storm time disturbance electric fields. The anomalies between the GAGAN TEC and IGS TEC maps are discussed in terms of the possible limitations of the IGS TEC maps in capturing storm time EIA variability over the Indian region.

Keywords: Main phase step-I of the 2015 St. Patrick's Day storm; Equatorial ionization anomaly; Storm time disturbance electric fields

1. Introduction

Electrodynamical coupling between high and low latitudes during geomagnetic storms causes the low latitude ionosphere to behave chaotically on a global scale. The low latitude ionospheric electric field is subjected to change due to the prompt penetration electric field (PPE) and/or disturbance dynamo electric field (DDE) during geomagnetic storms. PPE is solar wind/magnetosphere originated electric field which maps to high latitudes and penetrates almost instantaneously to low latitudes (Nishida, 1968; Vasyliunas, 1970). The resultant effect can perturb the low latitude ionospheric electric field within few minutes and up to an hour after the sudden storm commencement (SSC). The maximum energy transfer during a storm occurs when interplanetary magnetic field (IMF) Bz is southward. PPE, in general, is further divided into convection and overshielding electric fields (Fejer et al., 1979). The convection electric field occurs mostly during main phase of the storm while the later occurs during recovery phase of the storm (e. g. Kikuchi et al., 2008). Penetration

* Corresponding author.
E-mail address: bagiyamala@gmail.com (M.S. Bagiya).

http://dx.doi.org/10.1016/j.asr.2017.06.010
0273-1177/

of the convection electric field from high to low latitudes depends on the shielding that inner magnetosphere provides to low latitudes. Generally, the convection field is from dawn-to-dusk on the dayside and dusk-to-dawn on the nightside.

The inner magnetosphere sets up the polarization charges which give rise to dusk-to-dawn shielding electric field at the inner edge of the ring current (e.g. Kelley et al., 1979; Huang et al., 2005; Wolf et al., 2007; Bhaskar and Vichare, 2013). When the shielding electric field is high, the dusk-to-dawn electric field is observed at low latitudes which is known as overshielding whereas when the shielding electric field is less, the dawn-to-dusk electric field is observed at low latitudes which is known as undersheilding. The dawn-to-dusk PPE manifests as eastward electric field on the dayside ionosphere, thus enhances the background ionospheric electric field. The daytime PPE effects could be directly observed from equatorial electrojet (EEJ) measurements (e.g. Tsurutani et al., 2004; Bagiya et al., 2011). On other side, the dusk-to-dawn PPE manifests as westward electric field and thus weakens the background ionospheric electric field. Using EEJ observations, many studies have shown the penetration of dusk-to-dawn PPE during northward turning of IMF Bz (e. g. Rastogi and Patel, 1975; Fejer et al., 1979; Kelley et al., 2003; Huang et al., 2007; Wei et al., 2011; Simi et al., 2012). Kelley et al. (1979) reported that dusk-to-dawn electric field during northward IMF Bz is mainly due to the overshielding effect. They stated that during northward turning of IMF Bz, reconnection occurs in a narrow latitude belt at the edges of the polar cap. Thus, the direct penetration of dusk-to-dawn electric field may not be efficient. Daytime PPE effect, during southward IMF Bz condition, adds up to the ionospheric dynamo electric field and enhances the upward vertical plasma drift which raises the equatorial and low-latitude ionospheric plasma to higher altitudes where recombination rate is slow. This results into the enhanced ionospheric electron density and strong equatorial ionization anomaly (EIA) in the dayside sector (e.g. Maruyama et al., 2004; Tsurutani et al., 2004; Lin et al., 2005; Mannucci et al., 2005; Zhao et al., 2005; Balan et al., 2010; Bagiya et al., 2011, 2014 and references there in).

DDE is slowly varying and associated with the storm time meridional circulation from polar to equatorial latitudes that perturbs the low latitude ionosphere during and up to about a day or two after the onset of a geomagnetic storm (Blanc and Richmond, 1980). The Joule heating is one of the potential atmospheric energy source during geomagnetic storm (Fuller-Rowell et al., 1994, 1996). The storm time excess energy deposition at high latitudes enhances the Joule heating that induces an equatorward meridional wind and such a wind in conjunction with background wind changes the neutral wind circulation globally (e.g. Fuller-Rowell et al., 1994, 1996; Bagiya et al., 2014). The circulation of storm induced disturbed winds gives rise to an electric field which is westward on dayside thus reduces the ambient ionospheric electric field and eastward in post-midnight to pre-sunrise hours. DDE effects cause the depletion of daytime ionospheric electron density and also suppresses the EIA development (e.g. Tsurutani et al., 2004; Bagiya et al., 2011 and references therein).

In brief, the low latitude ionospheric plasma significantly deviates from its quiet day's pattern under the effects of varying storm time disturbance electric fields. The low latitude ionospheric response to any storm depends on several factors like intensity and duration of the storm, local occurrence time and also season (e.g. Pallamraju et al., 2004; Bagiya et al., 2014). In this line, the present study reports the dayside low latitude ionospheric variability in terms of EIA evolution across the India longitudes during the moderate main phase step-I of the recent 2015 St. Patrick's Day storm. The 17 March 2015 storm is the most intense storm of solar cycle 24 so far. Therefore, it has received conspicuous attention from the scientific community working in the field of equatorial-low latitude ionosphere. Several observational and modeling studies pertaining to the effects of this storm on the global as well as regional ionosphere-thermosphere system are well documented (e.g. Astafyeva et al., 2015; Carter et al., 2016; Chen et al., 2016; Liu et al., 2016; Ramsingh et al., 2015; Zhang et al., 2015; Kalita et al., 2016; Nava et al., 2016; Zakharenkova et al., 2016; Zhong et al., 2016; Ray et al., 2017; Huba et al., 2017). The present paper shows TEC observations made by the GPS Aided GEO Augmented Navigation (GAGAN) receivers over the Indian (northern EIA) region during the moderate main phase step-I of this storm. The total duration of the main phase step-I is around ∼6 h. Low latitude TEC over the Indian region are found to vary largely in terms of strengthening and weakening of EIA during this period. These TEC variations are discussed in terms of the varying storm time disturbance electric fields. This sort of in-depth study for the Indian low latitude ionosphere during the proposed storm period is not performed so far as per our knowledge. In addition, the present study also assesses the efficacy of the International GNSS service (IGS) TEC maps over the Indian region during a storm by comparing the evolution of storm time EIA across the Indian longitudes captured by IGS TEC maps with GAGAN-TEC observations.

2. Interplanetary, ring current and auroral ionospheric observations during 17 March 2015 storm

The interplanetary magnetic field (IMF) Bz component, dawn to dusk component of interplanetary electric field (IEFy), symmetric ring current (SYM-H) index and auroral electrojet (AE) index are shown in Fig. 1a during 17–18 March 2015 to represent the storm. IMF Bz turns southward at ∼0605 UT. The disturbances in IEFy, SYM-H index and AE index are observed almost simultaneously with this. The magnetic activity at high latitudes is moderate during initial period of the storm and the corresponding

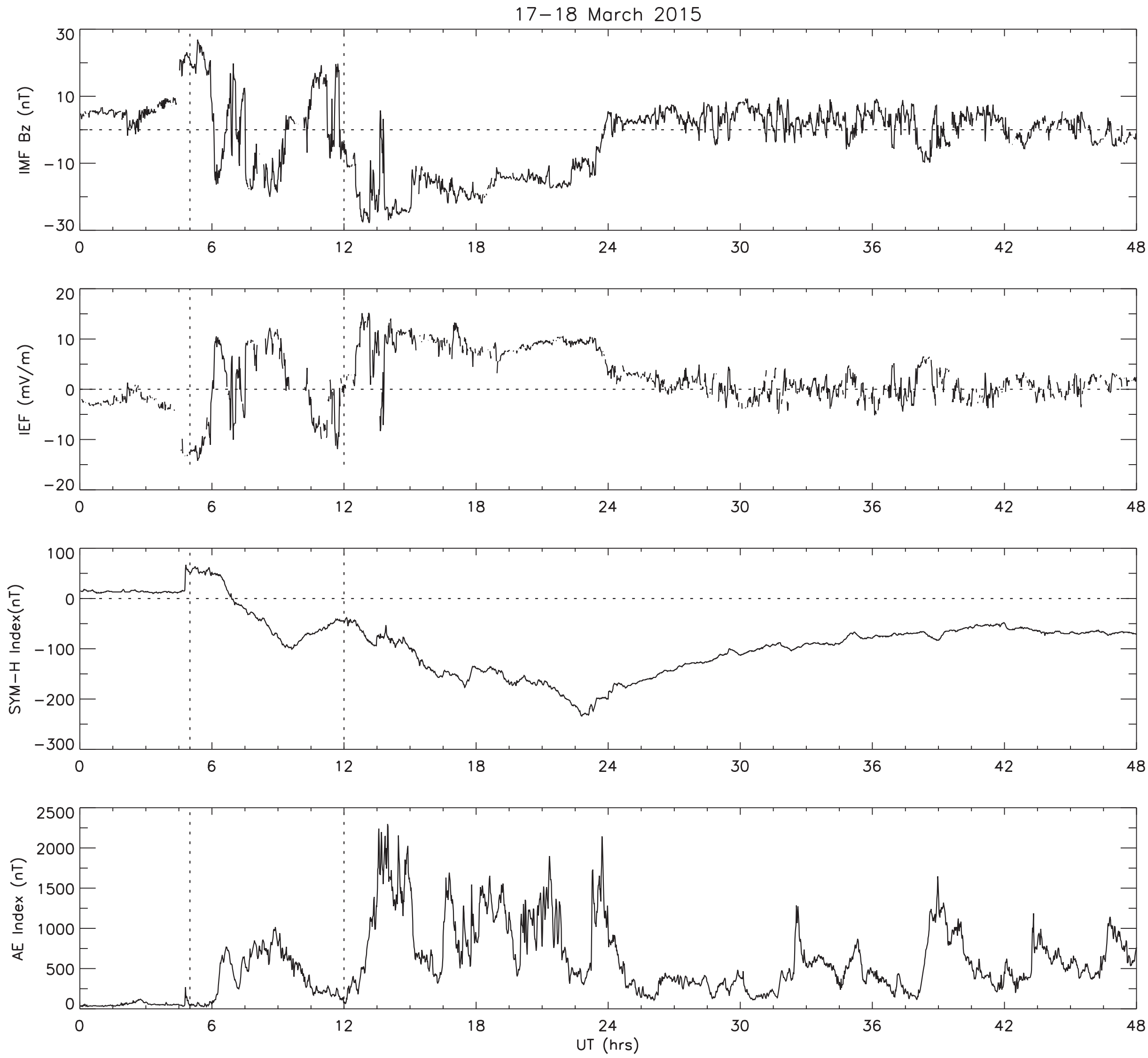

Fig. 1a. Variability of interplanetary (IMF Bz, IEFy), magnetospheric (SYM-H) and ionospheric (AE) parameters during 17–18 March 2015. From top (a) north-south component of interplanetary magnetic field (IMF) Bz (b) dawn to dusk component of interplanetary electric field (IEFy) (c) symmetric ring current (SYM-H) index and (d) auroral electrojet (AE) index during 17–18 March 2015. The storm main phase occurred in two steps. The moderate storm activity during main phase step-I between 0600 to 1200 UT is mainly focused here. The main phase step-I is highlighted in Fig. 1a with dashed vertical lines and shown separately in Fig. 1b for better clarity.

SYM-H variations also reports a moderate storm (minimum SYM-H of ∼−101 nT). The southward turning of IMF Bz at ∼1145 UT, that followed by the intense activity at high latitudes, results into the geomagnetic storm with second step development of main phase in SYM-H which has minimum of ∼−234 nT at ∼2248 UT on 17 March. The SYM-H variations imply that the storm main phase occurred in two steps [e.g. Kamide and Kusano, 2015]. The recovery phase of the storm starts after this as could be seen in Fig. 1a. We mainly focus on the moderate storm activity between 06 to 12 UT i.e. main phase step-I that coincides with the dayside over the Indian sector. The main phase step-I is highlighted in Fig. 1a with dashed vertical lines and shown separately in Fig. 1b for better clarity.

3. Ionospheric observations

GPS-TEC observations from GAGAN stations and IGS TEC maps serve the main database for the present study. The locations of GAGAN stations are shown in Fig. 2 and also listed in Table 1. TEC estimation method and removal of biases for GAGAN stations is explained in Rajat et al. (2007). The IGS TEC maps are derived by the IGS iono working group using the global IGS TEC observations. In the present study, TEC maps with time resolution of 15 min are considered (http://cdaweb.gsfc.nasa.gov). In maps, TEC is estimated as vertical TEC at grid points arranged every 2.5° of latitudes and 5° of longitudes in the latitude span of −87.5° to +87.5° and longitude span

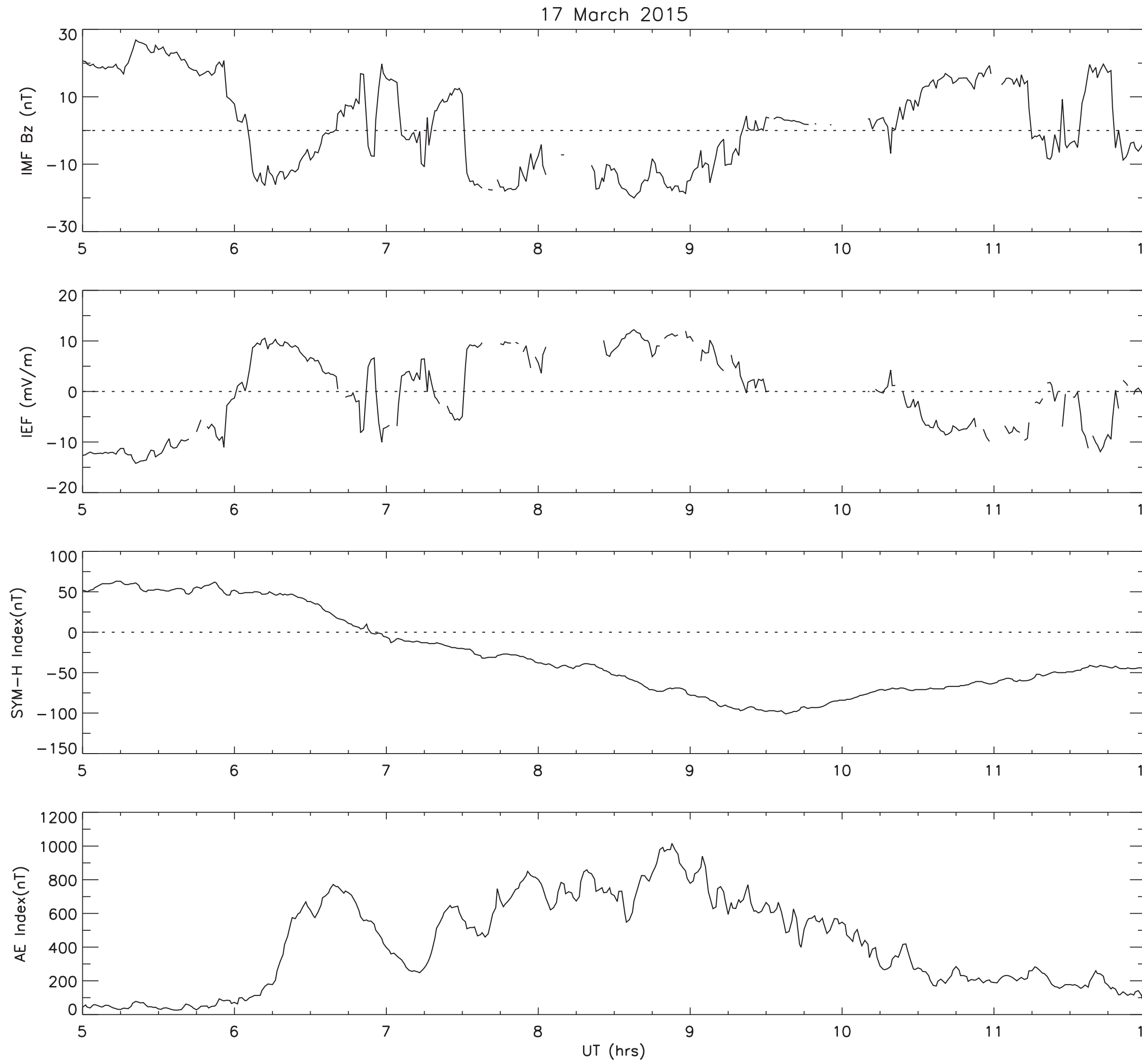

Fig. 1b. Same as Fig. 1a but mainly shows variability during main phase step-I between 0600 and 1200 UT (highlighted portion in Fig. 1a).

of −180° to +180° respectively. Thus, the global grid consists of 71 latitudes × 73 longitudes. The elevation cut off for map TEC is 10°. Each map in turn provides a snapshot of global ionosphere at given epoch [Feltens and Schaer, 1998; Wienia, 2008]. The IGS TEC map outputs within latitude zone of 5° to 30°N and longitude zone of 65°E to 95° E, mainly the Indian region, are considered here. It has to be noted that presently only three IGS stations are available over the India region. These stations locations are shown in Fig. 1 and also listed in Table 1. In order to compare the GAGAN derived TEC to that of the map output, similar elevation cutoff of 10° is used while deriving TEC from GAGAN stations.

EEJ is an indirect way to study the storm induced low latitude ionospheric electric field variability. The EEJ strength is derived here for the Indian sector using the variability of horizontal geomagnetic field at Alibag (18.46°N 72.87°E, magnetic latitude 10.19°N) and at Tirunelveli (8.70°N 77.80°E, magnetic latitude 0.03°N) as ($\Delta H_{(TIRUNELVELI)} - \Delta H_{(ALIBAG)}$) (Rastogi and Klobuchar, 1990).

4. Dayside low latitude ionospheric variability across the Indian longitudes during the main phase step-I of the 17 March 2015 geomagnetic storm

Dayside low latitude ionosphere is generally featured by EIA. EIA in general evolves during daytime and subsides during night. The diurnal variations of zonal ambient ionospheric dynamo electric field (eastward during daytime) control the evolution of EIA. The horizontal north-south geomagnetic field along with the eastward ambient dynamo electric field at geomagnetic equatorial latitudes lifts the F-region plasma vertically up under the effect of upward E × B drift. The plasma that is lifted to higher altitudes diffuses downward along the geomagnetic field lines under the

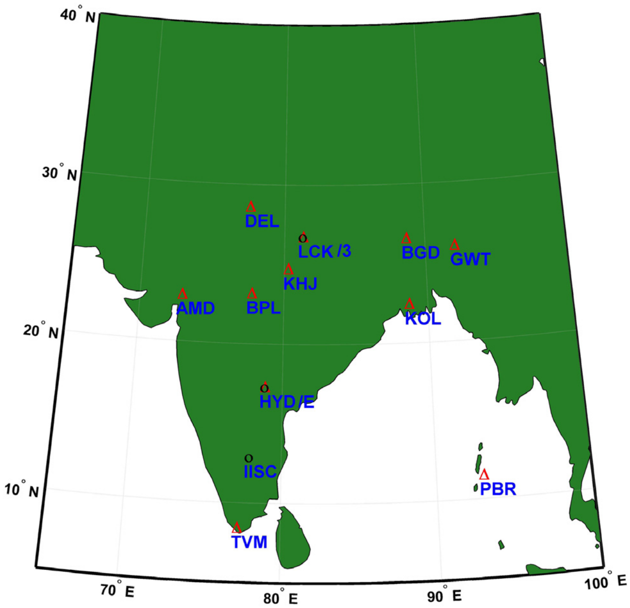

Fig. 2. Locations of GAGAN GPS (red triangle) and IGS stations (black circle) over the Indian region (for more details refer Table 1). (For interpretation of the references to colours in this figure legend, the reader is referred to the web version of this paper.)

Table 1
GAGAN and IGS GPS stations over the Indian region.

Station name	Latitude	Longitude
TRV	8.52	76.94
HYD	17.39	78.49
BPL	23.62	77.41
DEL	28.70	77.10
LCK	26.85	80.95
KHJ	24.83	79.92
BGD	26.70	88.31
KOL	22.57	88.36
GWT	26.14	91.74
PBR	11.62	92.73
AMD	23.02	72.57
IGS stations over the Indian region		
IISC	12.97	77.59
HYDE	17.39	78.49
LCK3	26.85	80.95

effects of gravity and pressure gradient forces. This phenomenon named as EIA and gives rise to depletion of plasma over the equator (trough) and two enhanced regions of plasma (crests) at ±15° of latitudes around the geomagnetic equator. The EIA crests and trough locations as well as the magnitude of EIA show significant day to day variability (e.g. Huang et al., 1989; Balan, 1995). Deshpande et al. (1977) showed the correlation between EEJ strength and development of EIA.

TEC observations from GAGAN GPS network provide an opportunity to observe the northern EIA evolution over the India sector. GAGAN TEC observations are validated for the diurnal, seasonal, solar cycle and geomagnetic storm time ionospheric variabilities over the Indian region [Rama Rao et al., 2006; Bagiya et al., 2009]. Thus, it can also serve as useful and handy tool to assess the efficacy of IGS TEC maps over the Indian region during geomagnetic storms. Before evaluating the IGS TEC maps during geomagnetic storms, it is first examined for one of the quiet days of March 2015. Fig. 3 shows TEC variations in GAGAN and IGS maps on 10 March (Ap = 4). It is to be noted here that observations from pbr (one of the GAGAN station) was not available for 10 March thus not included in Fig. 3. Top panel shows IGS TEC maps over the Indian region at four different epochs between 06 and 12 UT. TEC maps are shown in geographical latitudes and longitudes. The selected time window covers the local time of pre-noon to post-noon over the Indian region. Each maps shows variability for the duration of 15 min from the respective time indicated at the top of the map. In the bottom panel, TEC as observed by all satellites in view from the various GAGAN stations with elevation mask of 10° at every fifteen minutes are shown. The circles in bottom panel show the ionospheric piercing point locations of TEC measurements at the altitude of 450 km. The color shows the mangitude of TEC. The local time corresponds to a given longitude at a given UT is also shown in the bottom panel. The black dashed line shows the location of geomagnetic equator across the Indian longitudes. The geomagnetic latitudes are also shown in the figure with black solid lines. It could be observed from the figure that GAGAN TEC and IGS TEC maps show good agreement in dayside TEC variability over the Indian region on geomagnetically quiet day. In general, EIA crests response to the dynamo changes in about 2 to 3 h (Deshpande et al., 1977). Thus, the present approach of quiet day TEC examination at every two hours holds good for monitoring the EIA evolution. Except the strength discrimination, IGS TEC maps could capture the quiet day EIA evolution fairly well. The maps underestimate the TEC at EIA crest.

The EEJ strength between 0600 and 1300 UT, during main phase step-I, is derived and shown in Fig. 4 (solid line) along with the five quiet day's EEJ average (dashed line) from the similar month. The IEFy fluctuations are also shown in the figure for the same time window. It could be seen that on 17 March, EEJ responded significantly to the main phase step-I with sharp increase in strength (~55 nT) at ~0615 UT following the southward turning of IMF Bz and overshooting of IEFy at ~0605 UT (Fig. 1b). It could be noticed that further EEJ fluctuations more or less follows the IEFy variations pattern. The strong counter electrojet (CEJ) in EEJ is attributed to the northward turning of IMF Bz at 0918 UT (Fig. 1b). A gradual recovery in CEJ observed later.

TEC variations from the GAGAN stations during the main phase step-I of the storm are shown in Figs. 5–7 (top panel) at every 15 min along with the IGS TEC maps (bottom panel). Other information in Figs. 5–7 are same as that of Fig. 3.

As mentioned, the storm started with IMF Bz southward turning at ~0605 UT. Fig. 5a presents TEC varia-

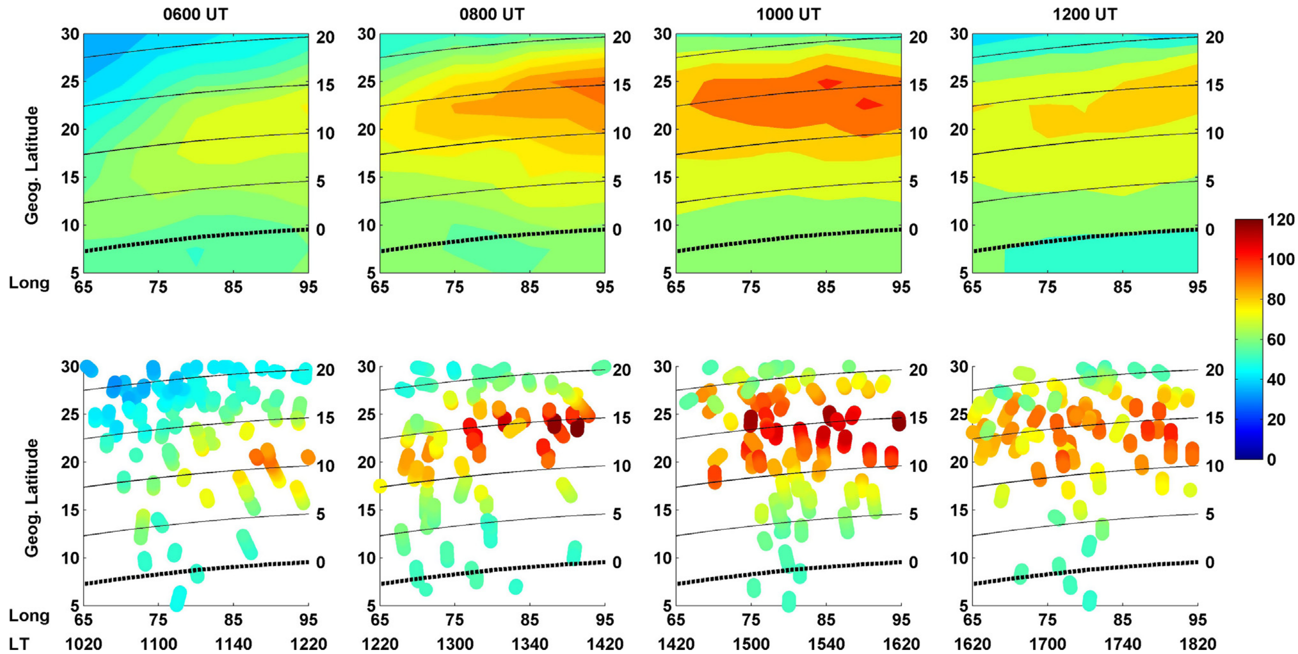

Fig. 3. Dayside low latitude ionospheric variability as observed by IGS TEC maps (top panel) and GAGAN TEC (bottom panel) on 10 March, one of the quiet days of March 2015. The location of geomagnetic equator across Indian longitudes is shown with dashed line. Solid lines show the geomagnetic latitudes. Local time corresponding to the given longitude at given UT is shown in each map (pls refer text for more details).

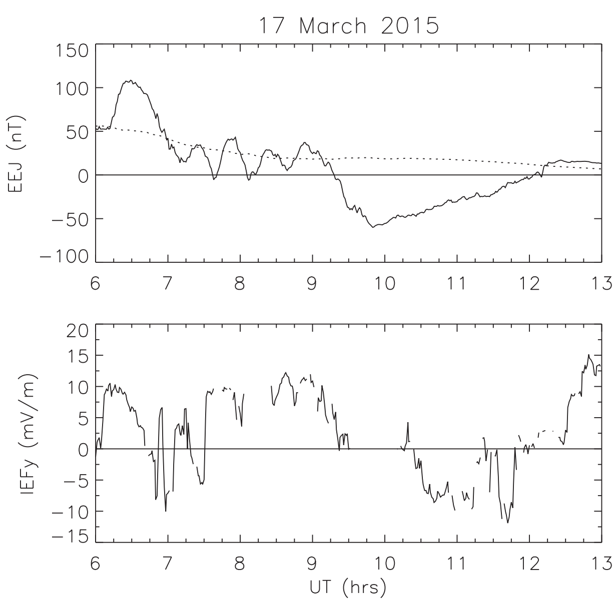

Fig. 4. Top panel shows EEJ variability during main phase step-I on 17 March 2015 (solid line) along with the five quiet day's EEJ average (dashed line) from the similar month. Bottom panel shows the IEFy fluctuations.

tions between 0615 and 0700 UT. It could be seen that TEC exhibits relatively moderate EIA before the storm. Following the storm onset at ~0605 UT, the GAGAN TEC enhances gradually. On the other hand the IGS maps could not show the similar TEC enhancements. It could be noticed that as the longitudes enter in post-noon hrs, the crest gradually develops with time and becomes more intense in GAGAN TEC. However, this feature is absent in IGS TEC maps. Though TEC map and GAGAN TEC show good agreement in latitudinal extent of EIA, GAGAN TEC exhibits more intense EIA crest. Between 0715 and 0745 UT (Fig. 5b), EIA becomes stronger and also farther extends latitudinally in GAGAN TEC, particularly over the longitude of post- noon hours while in the maps crest weakens. The longitudes of pre-noon sector exhibit reduction in GAGAN TEC. Significant TEC enhancement is observed over the entire region between 0800 UT and 1000 UT (Fig. 6a, b). The enhancements are more or less comparable both in GAGAN TEC and IGS maps except for the location of EIA crest. TEC in IGS maps significantly deviates from GAGAN TEC around EIA crest latitudes. After 1015 UT, EIA starts receding and becomes weak in TEC maps while the similar is observed in GAGAN TEC after 1045 UT (Fig. 7a). Also TEC at equatorward latitudes shows increase with this. The well evolved EIA crest disappears by 1130 UT both in TEC maps and GAGAN TEC (Fig. 7b). The resurgence of EIA is clearly observed in GAGAN TEC between 1145 and 1200 UT but the maps are failed in showing this (Fig. 7b).

5. Discussion and summary

The longitudes of 65°E (LT = UT + 0420 h) to 95°E (LT = UT + 0620 h) fall under the pre-noon to post-noon hrs during the main phase step-I. Thus, the Indian sector is an appropriate location to study the dayside low latitude ionospheric variability during the moderate main phase step-I of this large storm. The PPE effects that

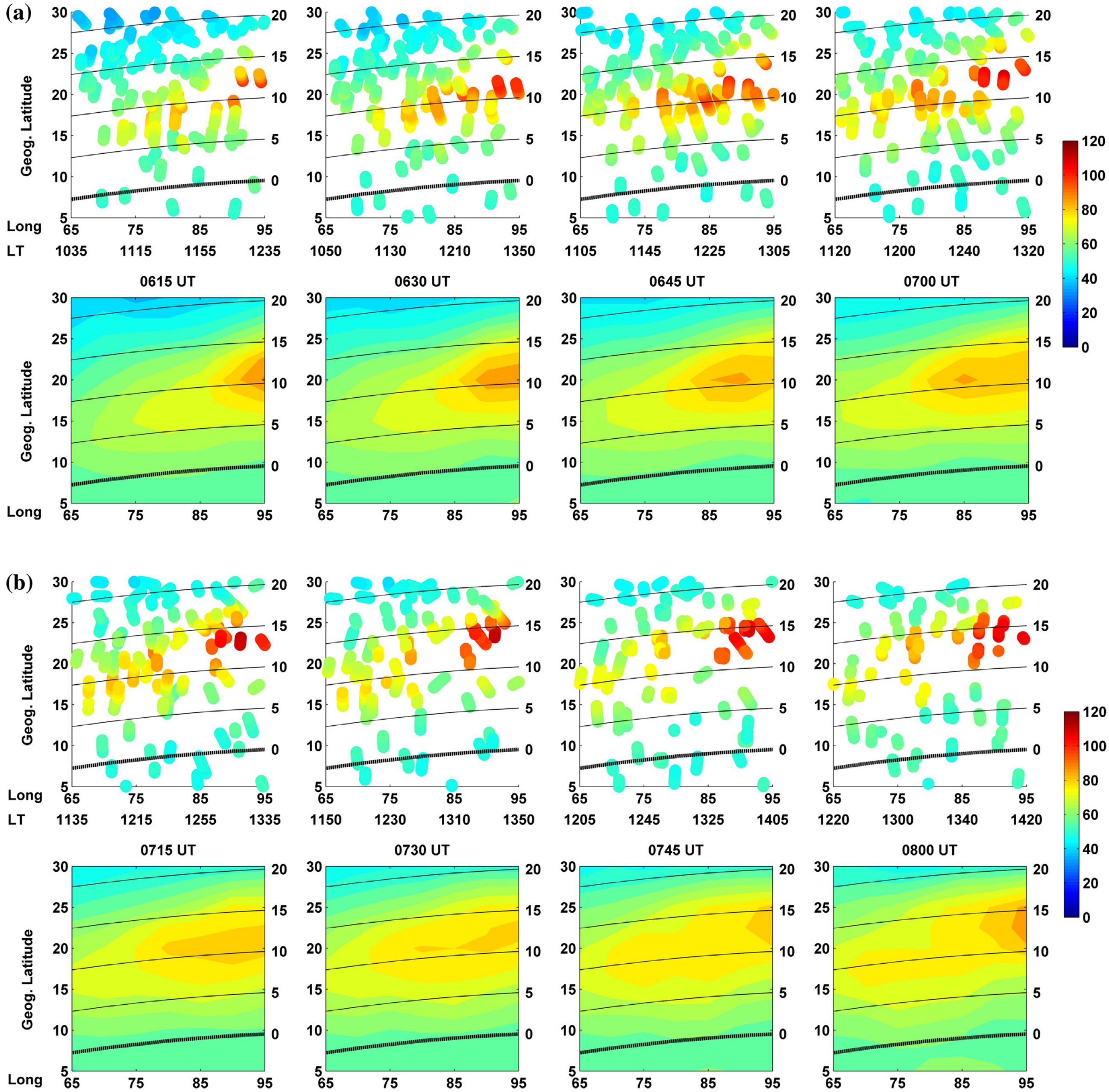

Fig. 5. (a) GAGAN TEC variations between 0615 to 0700 UT on 17 March 2015 (top panel). IGS TEC maps between 0615 and 0700 UT on the same day (bottom panel). (b) Same as Fig. 5(a) but time period is 0715 to 0800 UT. Other nomenclatures are same as in Fig. 3. Low latitude TEC across the Indian longitudes gradually enhances with the storm commencement. GAGAN TEC shows the enhancement more pronouncedly compare to IGS TEC maps.

accompanied the southward turning of IMF Bz ~605 UT are seen as low latitude TEC enhancements as exhibited by GAGAN TEC. In the dayside ionosphere, the PPE effect augments the ambient ionospheric dynamo electric field. This enhances the vertical upward drift and raises the plasma to higher altitudes where recombination rate is small, thereby enhances the total plasma density. GAGAN TEC behavior during the initial hours of storm commencement conveys that F-region moved to higher altitudes in the region of reduced recombination rate, under the effect of storm time PPE. Over the equator, this effect is stronger compared to low latitudes due to the high ambient dynamo field. The higher the eastward electric field, the larger would be the upward plasma drift. The higher the plasma moves over the equator, the farther it diffuses along the geomagnetic field lines under the fountain effect. Large shoot up in EEJ of ~55 nT at ~615 UT clearly indicates the effects of PPE over this region at this time. It is understood that during geomagnetic storms, the EEJ responds directly to PPE and indirectly to DDE and EIA requires 2 to 3 h to show the effects of modified dynamo region electric field. The observed intensified EIA both in GAGAN TEC and TEC maps after 0900 UT corroborates this (Figs. 5–7). Though the maps could

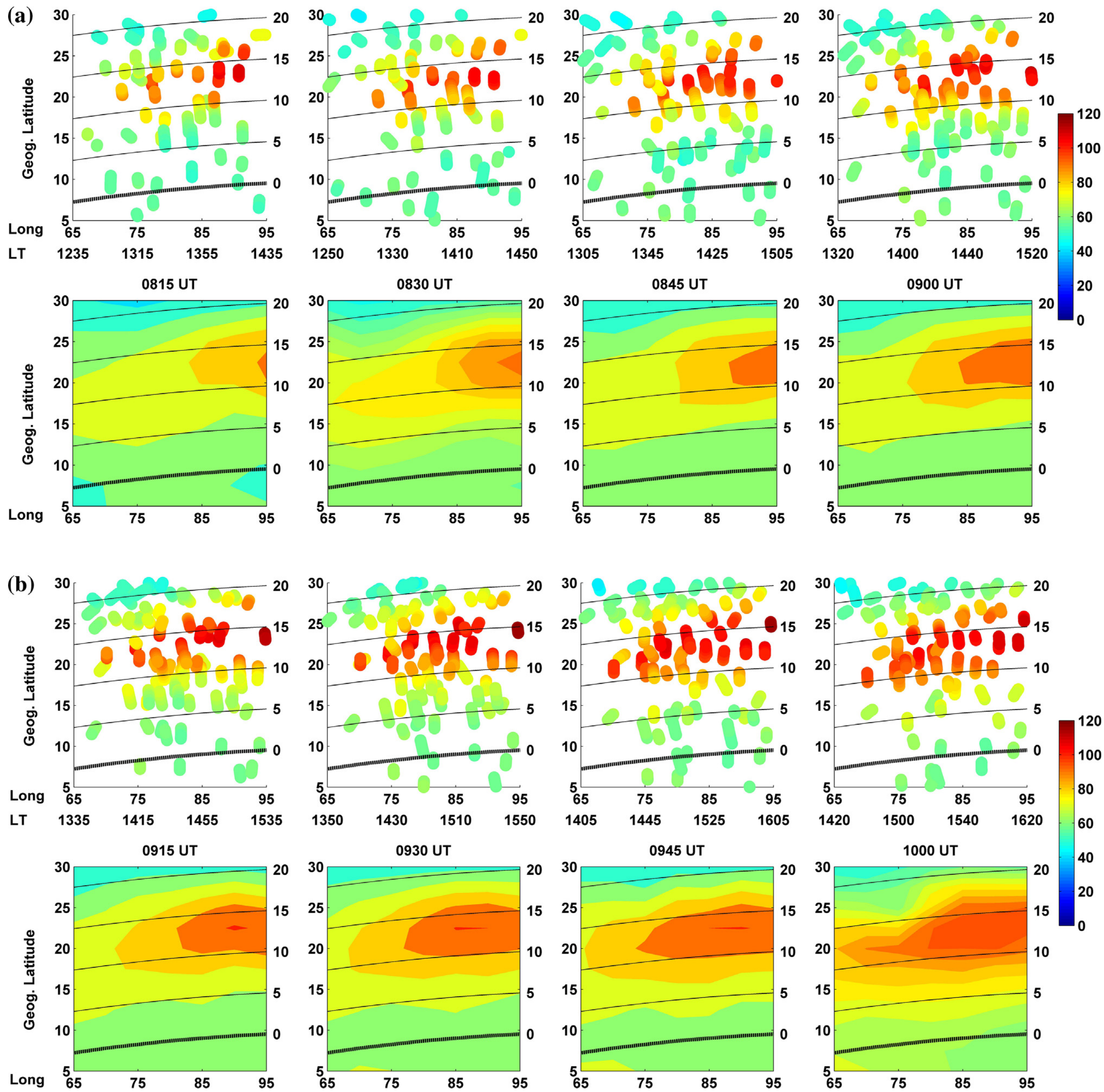

Fig. 6. (a) Same as Fig. 5 but time period is 0815 to 0900 UT. (b) Same as Fig. 5 but time period is 0915 to 1000 UT. GAGAN TEC exhibits more intense EIA evolution compare to IGS TEC maps but the latitudinal extent of EIA are comparable in both.

exhibit the storm time dynamics of EIA, the crest magnitudes are consistently underestimated by the maps.

The northward turning of IMF Bz ~918 UT has substantial effect on the dayside low latitude TEC on the storm day. Northward turning of IMF Bz reduces the convection electric field and enhances the overshielding field which is usually westward and in opposition to the daytime ionospheric dynamo electric field. In Fig. 4, the overshielding electric field reduces EEJ to large negative values. The effects of DDE could also be one of the potential candidates that can reduce the ambient dynamo electric field during daytime. But the effects of DDE over low latitude can be deciphered more effectively if the disturbances are followed by magnetically quiet period (Fejer et al., 1983). If magnetic disturbances are continued, the DDE effects may be obscured by PPE that occurs almost at the same time. In the present case, the main phase step-I is followed by a large step-II thus it is assumed that DDE effects are less here. The weakening of EIA in GAGAN TEC after 1045 UT clearly shows the effects of westward electric field over the Indian sector. This westward electric field penetration is attributed to the overshielding electric field associated with the northward turning of IMF Bz. The time delay of ~115 h between the northward turning of IMF Bz and the weakening of dayside low latitude ionosphere in GAGAN TEC strongly suggest that the overshielding

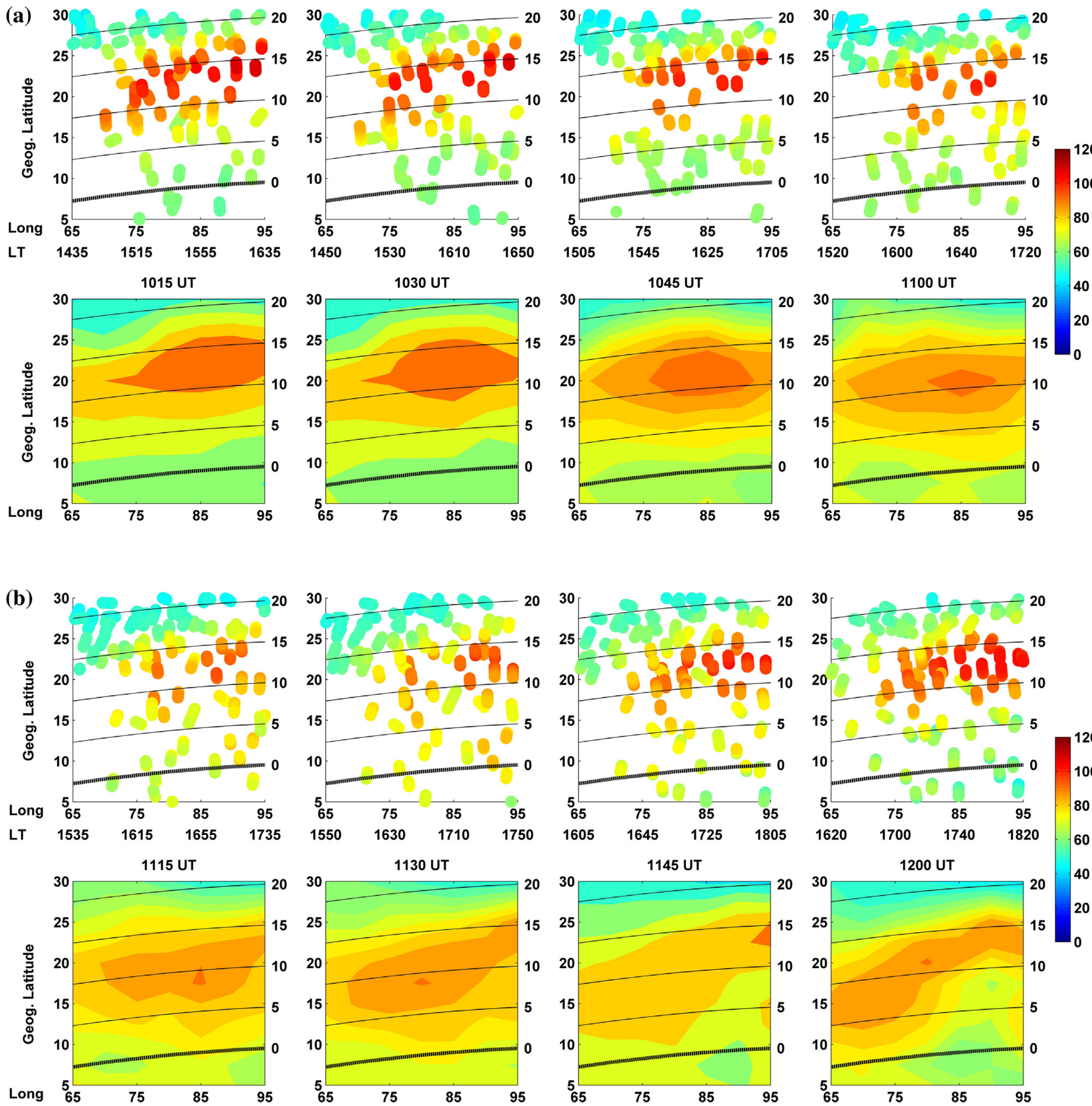

Fig. 7. (a) Same as Fig. 5 but time period is 1015 to 1100 UT. (b) Same as Fig. 5 but time period is 1115 to 1200 UT. The well evolved EIA weakens in IGS TEC maps after ∼45 min (i.e. ∼1015 UT) of the occurrence of the overshielding effect. In contrary, GAGAN TEC shows the corresponding feature after 1045 UT. Following the PPE at ∼1115 UT, GAGAN TEC shows resurgence of EIA but IGS TEC maps could not capture this feature.

effect dominates here. The receding of EIA is seen in both GAGAN TEC and IGS TEC maps. The receding EIA got reinvigorated under the effects of eastward PPE that accompanied with the southward turning of IMF Bz at ∼1113 UT. TEC observations, presented here, indicate that low latitude TEC varied significantly in response to the varying storm time disturbances electric fields during the main phase step-I of 17 March 2015 storm.

The GAGAN TEC and IGS TEC maps deviate significantly near the EIA crest but are in good agreement at other latitudes during the proposed storm period. In addition, TEC maps fail to show the renewal of EIA in evening hrs. Despite this it should be noted that the maps could successfully exhibit the effects of PPE and overshielding electric fields. The main reasoning behind the observed discrepancy could be the less number of IGS TEC observable stations (presently three) over the Indian longitudes. Further, the mapping function that used in these maps seems to be appropriate for other latitudes than those of EIA crest latitudes. For EIA crest latitudes its performance is poor during both quiet as well as storm day. It is observed that EIA peaks after ∼14:00 LT at corresponding longitudes in all TEC maps. No doubt, this is what usually expected. But during geomagnetic storms, EIA could occur earlier/later depending on the prevailing electrodynamical changes. Thus, the model has to be updated for local time variations of EIA particularly during storms. Though the EIA latitudinal extent is comparable on both quiet and storm days but it should also be noted that the presently observed EIA extent occurred during moderate storm activity. During major storms the EIA may extend to more higher latitudes. We may have to check this aspect in TEC maps for major storm activity too. The modest attempt of evaluating IGS TEC maps over the Indian region using the actual TEC observations leads to the inference that added caution must be taken into account while addressing storm time low latitude variability using IGS TEC maps.

Acknowledgements

The authors thank the Observational and Data Analysis (ODA) unit of Indian Institute of Geomagnetism for providing the EEJ strength data. The GAGAN GPS data are part of the GAGAN project, a joint collaboration between ISRO and Airports Authority of India. The authors acknowledge the NASA/GSFC CDAWeb for providing IGS TEC maps and the interplanetary data, WDC-C2 (Kyoto) for the auroral electrojet and geomagnetic indices data. This work is supported by Department of Science and Technology (DST), India. SS duly acknowledges the support of the Airport Authority of India.

References

Astafyeva, E., Zakharenkova, I., Forster, M., 2015. Ionospheric response to the 2015 St Patrick's day storm: A global multi-instrumental overview. J. Geophys. Res. Space Phys. 120, 9023–9037. http://dx.doi.org/10.1002/2015JA02629.

Bagiya, M.S., Joshi, H.P., Iyer, K.N., Aggarwal, M., Ravindran, S., Pathan, B.M., 2009. TEC variations during low solar activity period (2005–2007) near the equatorial ionospheric anomaly crest region in India. Ann. Geophys. 27, 1047–1057.

Bagiya, M.S., Iyer, K.N., Joshi, H.P., Thampi, S.V., Tsugawa, T., Ravindran, S., Sridharan, R., Pathan, B.M., 2011. Low-latitude ionospheric thermospheric response to storm time electrodynamical coupling between high and low latitudes. J. Geophys. Res. 116, A01303. http://dx.doi.org/10.1029/2010JA015845.

Bagiya, M.S., Hazarika, R., Laskar, F.I., Sunda, S., Gurubaran, S., Chakrabarty, D., Bhuyan, P.K., Sridharan, R., Veenadhari, B., Pallamraju, D., 2014. Effects of prolonged southward interplanetary magnetic field on low-latitude ionospheric electron density. J. Geophys. Res. Space Phys. 119, 5764–5776. http://dx.doi.org/10.1002/2014JA020156.

Balan, N., 1995. Modeling studies of the conjugate-hemisphere differences in ionospheric ionization at equatorial anomaly latitudes. J. Atmos. Sol. Terr. Phys. 57, 279–292.

Balan, N., Shiokawa, K., Otsuka, Y., Kikuchi, T., VijayaLekshmi, D., Kawamura, S., Yamamoto, M., Bailey, G.J., 2010. A physical mechanism of positive ionospheric storms at low latitudes and midlatitudes. J. Geophys. Res. 115, A02304. http://dx.doi.org/10.1029/2009JA014515.

Bhaskar, A., Vichare, G., 2013. Characteristics of penetration electric fields to the equatorial ionosphere during southward and northward IMF turnings. J. Geophys. Res. 118, 4696–4709. http://dx.doi.org/10.1002/jgra.50436.

Blanc, M., Richmond, A.D., 1980. The ionospheric disturbance dynamo. J. Geophys. Res. 85, 1669–1686.

Carter, B.A., Yizengaw, E., Pradipta, R., Retterer, J.M., Groves, K., Valladares, C., Caton, R., Bridgwood, C., Norman, R., Zhang, K., 2016. Global equatorial plasma bubble occurrence during the 2015 St. Patrick's Day storm. J. Geophys. Res. Space Phys. 121, 894–905. http://dx.doi.org/10.1002/2015JA022194.

Chen, C.H., Lin, C.H., Matsuo, T., Chen, W.H., 2016. Ionosphere data assimilation modeling of 2015 St. Patrick's Day geomagnetic storm. J. Geophys. Res. Space Phys. 121, 11549–11559. http://dx.doi.org/10.1002/ 2016JA023346.

Deshpande, M.R., Rastogi, R.G., Vats, H.O., Klobuchar, J.A., Sethia, G., Jain, A.R., Subbarao, B.S., Patawari, V.M., Janve, A.V., Rai, R.K., Singh, M., Gurm, H.S., Murthy, B.S., 1977. Effect of electrojet on the total electron content of the ionosphere over the Indian sub-continent. Nature 267, 599–600.

Fejer, B.G., Gonzales, C.A., Farley, D.T., Kelley, M.C., Woodman, R.F., 1979. Equatorial electric fields during magnetically disturbed conditions: 1. The effect of the interplanetary magnetic field. J. Geophys. Res. 84, 5797–5802. http://dx.doi.org/10.1029/JA084iA10p05797.

Fejer, B.G., Larsen, M.F., Farley, D.T., 1983. Equatorial disturbance dynamo electric fields. Geophys. Res. Lett. 10, 537–540. http://dx.doi.org/10.1029/GL010i007p00537.

Feltens, J., Schaer, S., 1998. IGS Products for the Ionosphere. In: Proceedings of IGS Analysis Centers Workshop.

Fuller-Rowell, T.J., Codrescu, M.V., Moffett, R.J., Quegan, S., 1994. Response of the thermosphere and ionosphere to geomagnetic storms. J. Geophys. Res. 99 (A3), 3893–3914. http://dx.doi.org/10.1029/93JA02015.

Fuller-Rowell, T.J., Codrescu, M.V., Moffett, R.J., Quegan, S., 1996. On the seasonal response of the thermosphere and ionosphere to geomagnetic storms. J. Geophys. Res. 101, 2343–2353. http://dx.doi.org/10.1029/95JA01614.

Huang, Y.N., Cheng, K., Chen, S.W., 1989. On the equatorial anomaly of the ionospheric total electron content near the northern anomaly crest. J. Geophys. Res. 94, 13 515–13 525.

Huang, C.M., Richmond, A.D., Chen, M.Q., 2005. Theoretical effects of geomagnetic activity on low- latitude ionospheric electric fields. J. Geophys. Res. 110, A05312. http://dx.doi.org/10.1029/2004JA010994.

Huang, C., Sazykin, S., Chau, J.L., Maruyama, N., Kelley, M.C., 2007. Penetration electric fields: efficiency and characteristic time scale. J. Atmos. Sol. Terr. Phys. 69, 1135–1146.

Huba, J.D., Sazykin, S., Coster, A., 2017. SAMI3-RCM simulation of the 17 March 2015 geomagnetic storm. J. Geophys. Res. Space Phys. 122, 1246–1257. http://dx.doi.org/10.1002/2016JA023341.

Kalita, B.R., Hazarika, R., Kakoti, G. et al., 2016. Conjugate hemisphere ionospheric response to the St. Patrick's Day storms of 2013 and 2015 in the 100°E longitude sector, J. Geophys. Res. Space Physics, 121, 11364–11390, http://dx.doi.org/10.1002/2016JA023119.

Kamide, Y., Kusano, K., 2015. No major solar flares but largest geomagnetic storm in the present solar cycle. Space Weather 13, 365–367. http://dx.doi.org/10.1002/2015SW001213.

Kelley, M.C., Fejer, B.G., Gonzales, C.A., 1979. An explanation for anomalous ionospheric electric fields associated with a northward turning of the interplanetary magnetic field. Geophys. Res. Lett. 6, 301–304. http://dx.doi.org/10.1029/GL006i004p00301.

Kelley, M.C., Makela, J.J., Chau, J.L., Nicholls, M.J., 2003. Penetration of the solar wind electric field into the magnetosphere/ionosphere system. Geophys. Res. Lett. 30 (4), 1158. http://dx.doi.org/10.1029/2002GL016321.

Kikuchi, T., Hashimoto, K.H., Nazoki, K., 2008. Penetration of magnetospheric electric fields to the equator during a geomagnetic storm. J. Geophys. Res. 113, A06214. http://dx.doi.org/10.1029/2007JA012628.

Lin, C.H., Richmond, A.D., Liu, J.Y., Yeh, H.C., Paxton, L.J., Lu, G., Tsai, H.F., Su, S.-Y., 2005. Large-scale variations of the low-latitude ionosphere during the October–November 2003 superstorm: Observational results. J. Geophys. Res., 110, A09S28, http://dx.doi.org/10.1029/2004JA010900.

Liu, J., Wang, W., Burns, A., Yue, X., Zhang, S., Zhang, Y., Huang, C., 2016. Profiles of ionospheric storm-enhanced density during the 17 March 2015 great storm. J. Geophys. Res. Space Phys. 121, 727–744. http://dx.doi.org/10.1002/2015JA021832.

Mannucci, A.J., Tsurutani, B.T., Iijima, B.A., Komjathy, A., Saito, A., Gonzalez, W.D., Guarnieri, F.L., Kozyra, J.U., Skoug, R., 2005. Dayside global ionospheric response to the major interplanetary events of October 29–30, 2003 "Halloween Storms", Geophys. Res. Lett., 32, L12S02, http://dx.doi.org/10.1029/2004GL021467.

Maruyama, T., Ma, G., Nakamura, M., 2004. Signature of TEC storm on 6 November 2001 derived from dense GPS receiver network and ionosonde chain over Japan. J. Geophys. Res. 109, A10302. http://dx.doi.org/10.1029/ 2004JA010451.

Nava, B., Rodríguez-Zuluaga, J., Alazo-Cuartas, K., Kashcheyev, A., Migoya-Orué, Y., Radicella, S.M., Amory-Mazaudier, C., Fleury, R., 2016. Middle and low latitude ionosphere response to 2015 St. Patrick's Day geomagnetic storm. J. Geophys. Res. Space Phys. 121, 3421–3438. http://dx.doi.org/10.1002/ 2015JA022299, in the Journal of Geophysical Research - Space Physics, Special issue on Big Storms, 2016.

Nishida, A., 1968. Geomagnetic DP2 fluctuations and associated magnetospheric phenomena. J. Geophys. Res. 73, 1795–1803. http://dx.doi.org/10.1029/JA073i005p01795.

Pallamraju, D., Chakrabarti, S., Valladares, C.E., 2004. Magnetic storm-induced enhancement in neutral composition at low latitudes as inferred by O(1D) dayglow measurements from Chile. Ann. Geophys. 22, 3241–3250.

Rama Rao, P.V.S., Gopi Krishna, S., Niranjan, K., Prasad, D.S.V.V.D., 2006. Temporal and spatial variations in TEC using simultaneous measurements from the Indian GPS network of receivers during the low solar activity period of 2004–2005. Ann. Geophys. 24, 3279–3292.

Ramsingh, Sripathi, S., Sreekumar, S., Banola, S., Emperumal, K., Tiwari, P., Kumar, B.S., 2015. Low-latitude ionosphere response to super geomagnetic storm of 17/18 March 2015: Results from a chain of ground-based observations over Indian sector. J. Geophys. Res. Space Phys. 120, 10864–10882, http://dx.doi.org/10.1002/2015JA021509.

Rajat, A., Nagori, N., Jain, N., Suda, S., Regar, S., Sivaraman, M.R., Bandopadhyay, K., 2007. Ionospheric studies for the implementation of GAGAN. Ind. J. of Rad. Spa. Phy. 36, 394–404.

Rastogi, R.G., Klobuchar, J.A., 1990. Ionospheric electron content within the equatorial F_2 layer anomaly belts. J. Geophys. Res. 95, 19045–19052. http://dx.doi.org/10.1029/JA095iA11p19045.

Rastogi, R.G., Patel, V.L., 1975. Effect of interplanetary magnetic field on the ionosphere over the magnetic equator. Proc. Indian Acad. Sci. 82, 121–141.

Ray, S., Roy, B., Paul, K.S., Goswami, S., Oikonomou, C., Haralambous, H., Chandel, B., Paul, A., 2017. Study of the effect of 17–18 March 2015 geomagnetic storm on the Indian longitudes using GPS and C/NOFS. J. Geophys. Res. Space Phys. 122, 2551–2563. http://dx.doi.org/10.1002/2016JA023127.

Simi, K.G., Thampi, S.V., Chakrabarty, D., Pathan, B.M., Prabhakaran Nayar, S.R., Pant, T.K., 2012. Extreme changes in the equatorial electrojet under the influence of interplanetary electric field and the associated modification in the low-latitude F region plasma distribution. J. Geophys. Res. 117, A03331. http://dx.doi.org/10.1029/2011JA01732.

Tsurutani, B.T. et al., 2004. Global dayside ionospheric uplift and enhancement associated with interplanetary electric field. J. Geophys. Res. 109, A08302. http://dx.doi.org/10.1029/2003JA010342.

Vasyliunas, V.M., 1970. Mathematical models of the magnetospheric convection and its coupling to the ionosphere. In: McCormac, J.C. (Ed.), Particles and fields in the magnetosphere, 60–71, Springer, New-York, http://dx.doi.org/10.1007/978-94-010-3284-1-6.

Wei, Y., Wan, W., Pu, Z., Hong, M., Zong, Q., Guo, J., Zhao, B., Ren, Z., 2011. The transition to overshielding after sharp and gradual interplanetary magnetic field northward turning. J. Geophys. Res. 116, A01211. http://dx.doi.org/10.1029/2010JA015985.

Wienia, R.J., 2008. Use of global ionospheric maps for precise point positioning, MSc scriptie Delft University of Technology, the Netherlands.

Wolf, R.A., Spiro, R.W., Sazykin, S., Toffoletto, F.R., 2007. How the Earth's inner magnetosphere works: An evolving picture. J. Atmos. Sol. Terr. Phys. 69, 288–302.

Zakharenkova, I., Astafyeva, E., Cherniak, I., 2016. GPS and GLONASS observations of large-sc ale traveling ionospheric disturbances during the 2015 St. Patrick's Day storm. J. Geophys. Res. Space Phys. 121, 12138–12156. http://dx.doi.org/10.1002/2016JA023332.

Zhang, S.-R. et al., 2015. Thermospheric poleward wind surge at midlatitudes during great storm intervals. Geophys. Res. Lett. 42, 5132–5140. http://dx.doi.org/10.1002/2015GL064836.

Zhao, B., Wan, W., Liu, L., 2005. Response of equatorial anomaly to the October-November 2003 superstorm. Ann. Geophys. 23, 693–706. http://dx.doi.org/10.5194/angeo-23-693-2005.

Zhong, J., Wang, W., Yue, X., Burns, A.G., Dou, X., Lei, J., 2016. Long-duration depletion in the topside ionospheric total electron content during the recovery phase of the March 2015 strong storm. J. Geophys. Res. Space Phys. 121, 4733–4747. http://dx.doi.org/10.1002/2016JA022469.